International Journal of Heat and Mass Transfer 88 (2015) 945–956

Contents lists available at ScienceDirect

International Journal of Heat and Mass Transfer

journal homepage: www.elsevier.com/locate/ijhmt

Molten pool behaviors for second pass V-groove GMAW

Dae-Won Cho [a], Suck-Joo Na [b,*]

[a] Thermal Hydraulic Safety Research Division, Korea Atomic Energy Research Institute (KAERI), Daejeon, Republic of Korea
[b] Department of Mechanical Engineering, KAIST, Daejeon, Republic of Korea

ARTICLE INFO

Article history:
Received 15 October 2014
Received in revised form 6 May 2015
Accepted 6 May 2015
Available online 27 May 2015

Keywords:
Second pass welding
Gas metal arc welding
Computational fluid dynamics
Abel inversion
Volume of fluid
Positional welding
Convex bead
Concave bead

ABSTRACT

This study conducted three-dimensional transient numerical simulations for second pass gas metal arc welding on V-groove in various welding positions. To obtain arc models such as arc heat flux, electromagnetic force and, arc pressure, this study adopted the Abel inversion method and the resultant asymmetric arc models can be formed. Due to the different gravity effect, it is possible to obtain the different molten pool flow patterns, solidification times, temperature distributions and bead shapes along the welding positions by numerical simulations. The formation process of convex and concave weld bead has been analyzed in detail for different welding positions. The simulation results of the fusion zone were compared with the experimental ones; therefore, the various models used in this paper can be validated.

1. Introduction

In the welding process, the materials melt and solidify within a very short time. Moreover, it is very difficult to expect the weld bead shapes and the weld pool behavior because of the complex physical phenomena of the welding process. Many researches, therefore, expect the weld bead shapes to be formed by the welding parameters using statistical methods such as regression models [1,2] and neural networks [3–5].

However, developing numerical simulation methods with physical and practical welding models makes it possible to predict weld pool behaviors by computational fluid dynamics (CFD) simulations. Especially, the transient simulations with a volume of fluid (VOF) method described the more practical and meaningful weld pool can flow patterns [6–8]. Cao et al. showed the droplet impingement on the weld pool surface of the gas metal arc welding (GMAW) process [6]. Moreover, Cho and Na conducted laser-GMA hybrid welding, which combined the characteristics of the laser and GMAW without considering the mutual interaction effect between two welding processes [7]. Recently, the VOF transient simulation was applied to predict the alloying element distribution and pore formation in laser-arc hybrid welding [8]. However, the arc models used above did not seriously consider the size of the arc, so it is necessary to apply more realistic and physical arc models. Some studies have tried to obtain a distribution of the arc plasma [9,10]. Tsai and Eagar calculated the distribution of heat and current flux on an anode plate in gas tungsten arc welding (GTAW) process by using the Abel inversion method [9]. However, it takes a long to get the distribution parameters of the arc heat flux model. Cho and Na [10] proposed a robust and simple way to get the distribution of the arc plasma by using a matrix-calculated Abel inversion and a CCD camera. Moreover, this method can calculate the irradiance of axisymmetric and elliptically symmetric arc distributions, creating advanced development in the arc welding CFD simulations.

Cho et al. [11] made various arc models with an Abel inversion method and physical relations among the arc irradiance, arc temperature and arc current density. Further, they applied arc models such as arc heat flux, arc pressure, and electromagnetic models to CFD simulations for gas hollow tungsten arc welding (GHTAW) on bead-on plate. Similarly, many researchers calculated arc models by using a CCD camera and Abel inversion for various CFD welding cases. The Abel inversion method with a high speed camera brings many advantages to describe alternating current (AC) welding process where the size of the arc and signals (current and voltage) are different along time [12,13]. Cho et al. [12] captured various arc images which escaped from the flux within a very short time, and then made the transient arc models for the single electrode submerged arc welding (SAW) process. Kiran et al. [13] captured the arc images and derived arc interaction models for the

* Corresponding author.
E-mail address: sjoona@kaist.ac.kr (S.-J. Na).

http://dx.doi.org/10.1016/j.ijheatmasstransfer.2015.05.021

two-wire tandem SAW process with a physical relation between two arc plasmas. Moreover, Cho et al. [14] applied these advanced arc interaction models to a VOF transient CFD and then described the dynamic molten pool behaviors of the two-wire tandem SAW.

The gravity effect plays an important role in the molten pool flow because it is a body force throughout the entire domain. Therefore, the welding conditions should change along the various welding positions for pipe welding; otherwise, weld defects such as humping, melt-through, and lack of fusion can be formed. Cho et al. described these dynamic molten pool flow patterns on root pass GMA welding for various welding positions in VOF transient simulations [15].

This study calculated the arc models for 2nd pass GMAW with an Abel inversion method and described the various dynamic molten pool behaviors for different welding positions using commercial software, Flow-3D.

2. Theoretical formulation

2.1. Material shape and mesh size

Cho et al.[15] found that a high welding speed (20 mm/s) with a high current (spray mode of metal transfer) can bring a stable bead shape in a vertical downward position. With similar welding conditions in Table 1, it was found that bead shapes for the root pass welding in flat and overhead positions were stable and similar to each other, as shown in Fig. 1. Thus, this study used a shape for the material in 2nd pass GMAW, as shown in Fig. 2 and the experiment conditions for the 2nd pass GMAW, as written in Table 1. The mesh density used in the simulation was 0.25 mm/mesh to determine the molten pool behaviors because previous studies used at least four meshes for the droplet diameter [12,14–16]. All the simulations were conducted by transient numerical analysis. Welding started at 1.5 cm of the *x*-direction.

Table 1
Welding conditions for root pass welding.

Wire feed rate	8.2 m/min
Voltage	25 V
Electrode	YGW15, Φ = 1.2 mm
Current	260 A
Welding speed	20 mm/s (root pass) 10 mm/s (2nd pass)
CTWD	20 mm
Torch angle	90 degree
Shielding gas	80% Ar-20% CO2 20 l/min

2.2. Governing equations

The commercial software Flow-3D solved momentum, energy, mass conservation and VOF equations. The material properties used in this paper are listed in Table 2.

- Momentum equation –

$$\frac{\partial \vec{V}}{\partial t} + \vec{V} \cdot \nabla \vec{V} = -\frac{\nabla p}{\rho} + \frac{\mu}{\rho} \nabla^2 \vec{V} + \frac{\dot{m}_s}{\rho}(\vec{V}_s - \vec{V}) + f_b \tag{1}$$

- Mass conservation equation –

$$\nabla \cdot \vec{V} = \frac{\dot{m}_s}{\rho} \tag{2}$$

- Energy equation –

$$\frac{\partial h}{\partial t} + \vec{V} \cdot \nabla h = \frac{1}{\rho} \nabla \cdot (k \nabla T) + \dot{h}_s \tag{3}$$

where

$$h = \begin{cases} \rho_s C_s T & (T \leqslant T_s) \\ h(T_s) + h_{sl} \dfrac{T - T_s}{T_l - T_s} & (T_s < T \leqslant T_l) \\ h(T_l) + \rho_l C_l (T - T_l) & (T_l < T) \end{cases} \tag{4}$$

- VOF equation –

$$\frac{\partial F}{\partial t} + \nabla \cdot (\vec{V} F) = \dot{F}_s \tag{5}$$

2.3. Boundary conditions

The energy boundary condition on the top surface is considered by the arc heat flux and heat dissipation from convection, radiation and evaporation. The energy balance model on the top surface is expressed in Eq. (6).

$$k \frac{\partial T}{\partial \vec{n}} = q_A - q_{conv} - q_{rad} - q_{evap} \tag{6}$$

The pressure boundary on the free surface is applied as shown in Eq. (7).

$$p = p_A + \frac{\gamma}{R_c} \tag{7}$$

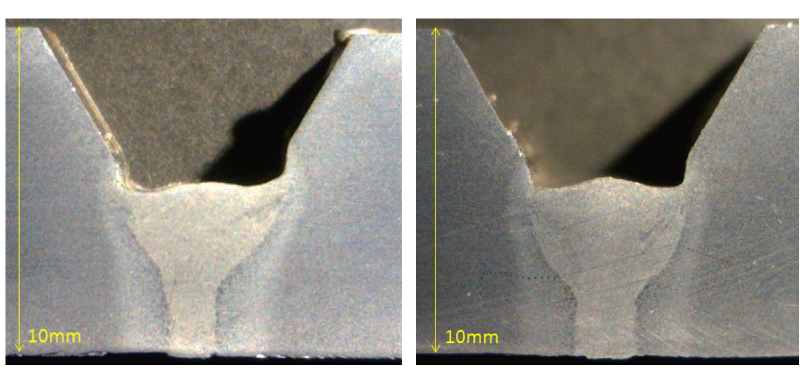

(a) Flat position (b) Overhead position

Fig. 1. Weld bead shapes of root pass welding with a high welding speed (20 mm/s).